WWJMRD 2026; 12(02): 10-16
www.wwjmrd.com
International Journal
Peer Reviewed Journal
Refereed Journal
Indexed Journal
Impact Factor SJIF 2017: 5.182 2018: 5.51, (ISI) 2020-2021: 1.361
E-ISSN: 2454-6615

Alfred Rufer
Faculty of Engineering
STI-DO
EPFL, Ecole Polytechnique
Fédérale de Lausanne
Station 11
CH1015 Lausanne

Correspondence:
Alfred Rufer
Faculty of Engineering STI-DO
EPFL Ecole Polytechnique
Fédérale de Lausanne
Station 11
CH1015 Lausanne
alfred.rufer@epfl.ch

Clutch Bearing Coupled PAM's (Pneumatic Artificial Muscle) for a Compressed Air Engine

Alfred Rufer

Abstract
A new compressed air engine is presented where the conversion from the thermodynamic level to mechanical motion is realized with pneumatic artificial muscles (PAMs). The engine architecture uses an original concept for the coupling of the PAM's to the engine axle based on freewheeling clutch bearings driven by short lever arms. The operation of the motor is described with a kinematic model which is further used for a numerical simulation. Forces, torque-contributions and mechanical power and work are represented related to the angular displacement of the motor shaft. The motor energetic efficiency is also evaluated. Finally, a physical experimental set-up has been realized for the verification of the concept.

Keywords: compressed air, pneumatic engine, pneumatic artificial muscle, efficiency

1. Introduction
Compressed air engines have been proposed in many contexts of use and in many different technologies. Their main advantages are in the simplicity and reliability of the technology, and in the acquisition costs of the equipments. Near standard industry applications in production of goods, handling or moving of objects, another application field in the energy sector concerns compressed air energy storage where conversion engines are used. Compressors are filling the storage reservoirs while in the recovery path expansion turbines or motors are placed between the storage vessel itself and the electrical generation machine [1]. The classical compressed air machines go from rotary vane type to piston/crankshaft types, through gear type or turbine type motors. In general, these motors have a low energetic efficiency due to their principle of conversion where only displacement work is produced in the machine [2-4]. Recent developments in the field of pneumatic to mechanical conversion allow to strongly increase the energetic performances of such machines. These benefits are realised through the addition to the conversion principle of a second torque component resulting from a real thermodynamic expansion inside of the active volume or in an added supplementary chamber of larger dimensions [5-8]. A new approach for the realization of compressed air engines has newly been presented where the pneumatic actuators are realized using so-called pneumatic artificial muscles (PAM) [9]. Pneumatic artificial muscles offer several advantages over conventional pneumatic cylinders: a high force-to-weight ratio, a flexible structure, minimal compressed air consumption, availability in various sizes, low cost, and high reliability. The low compressed air consumption is due to the small size of the pneumatic artificial muscle; thus, thanks to its high force-to-weight ratio, it can generate significant traction forces with minimal compressed air consumption [10-14]. The architecture of the engine described in [9] is a classical assembly using a crankshaft on which the artificial muscles are acting as connecting rods with variable length. Such a system has further been investigated in [15], where the operating principle and the intern variables as the forces developed by the muscles, the tangential force components acting on the crankpins, the developed torque and power have been described more in detail. Additionally, the energetic properties of such a system have been evaluated in terms of energy efficiency.
One of the typical properties of the artificial muscles is that their contraction length depends on the pressure of the injected air. Due to this specific behavior, the direct coupling of such

an actuator to the crankshaft with crankpins having a constant radius of gyration is not possible. In the original study of Reference 15 a solution using a so-called sliding anchor has been proposed, which solves the problem but makes the system more complex. In the present contribution an alternative solution to the classical crankshaft is proposed. In this solution the artificial muscles are driving the shaft of the engine with lever-arms which impose their sectorial rotation through freewheel clutch bearings [16]. The contraction motion of the muscles is driving the shaft while their relaxing movement is possible without any torque contribution, due to the freewheel effect of the clutch bearings. Figure 1 shows the specific engine architecture with the two coupled artificial muscles operating with 180° phase shift. On the lower left side of the figure the oscillating lever-arms can be seen. Their motion drives the outer rings of the clutch bearings while the inner rings are rigid against the engine shaft.

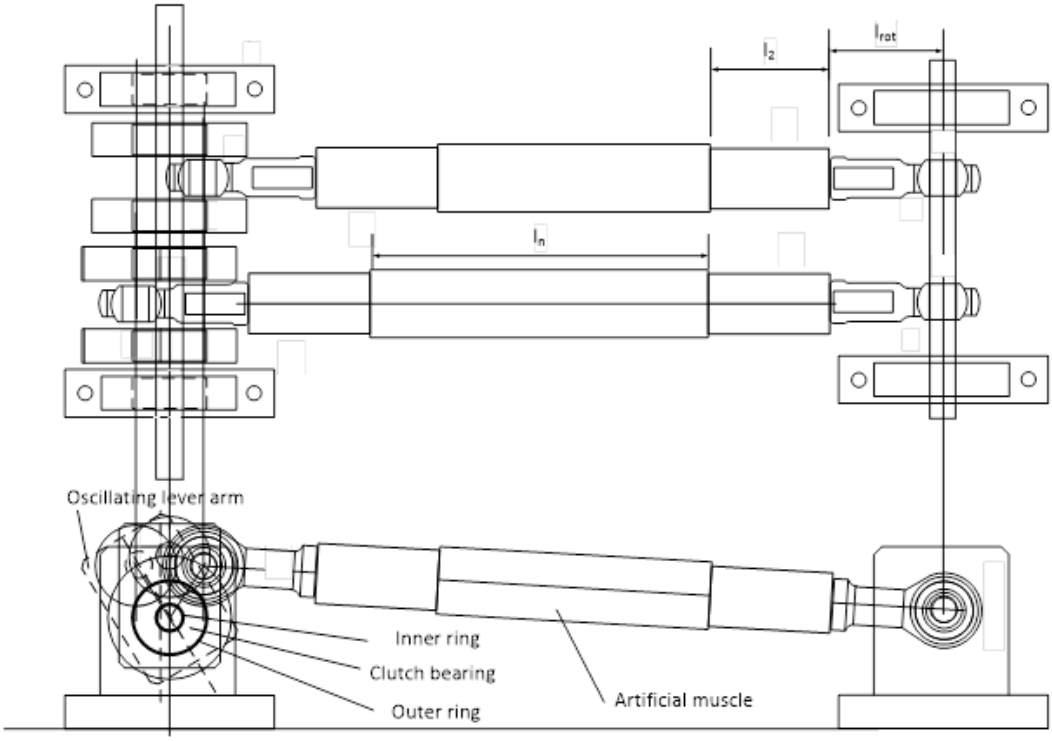

Fig. 1: Assembly of the proposed engine architecture.

2. Kinematic model of the engine

Figure 2 shows the geometric assembly of the motor with the main parameters. l_m represents the length of the active rod. For a relaxed state of the muscle, the length of the active rod takes the value of l_{m0}. l_{m0} is given by the nominal length of the active part of the muscle l_n completed by the length of the connecting elements (Relation 1). The distance between the anchor point of the active rod and the centre of the axis of the engine l_a is chosen according to Relation (2). In this relation the term $r \cdot \cos\varphi_0$ corresponds to half of the contraction length of the muscle (Relation 3) so that the oscillation of the lever arms is distributed symmetrically over the axis of the engine. And because the connection of the active rod to the lever arm needs sufficient space, the radius r (or the length of the lever arms) must be chosen accordingly. Depending on the value of Δl and the chosen radius r, the largest angle φ_0 is defined.

The length of the active rod l_m follows the rotation of the lever arm (Relation 4) and imposes the active length l_{eff} of the muscle (Relation 5).

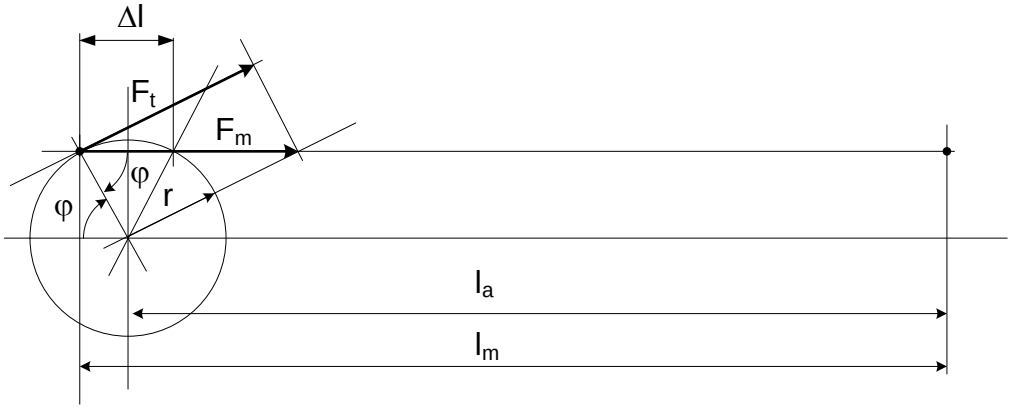

Fig. 2: Geometry and parameters of the engine.

$$l_{m0} = l_n + 2 \cdot l_2 + 2 \cdot l_{rot} = 0.1 + 0.072 + 0.072 = 0.244 \quad (1)$$

$$l_a = l_{m0} - r \cdot \cos\varphi_0 \quad (2)$$

$$r \cdot \cos\varphi_0 = \Delta l / 2 \quad (3)$$

$$l_m = l_a + r \cdot \cos\varphi = l_{m0} - r \cdot \cos\varphi_0 + r \cdot \cos\varphi \quad (4)$$

$$l_{eff} = l_n - r \cdot \cos\varphi_0 + r \cdot \cos\varphi \quad (5)$$

From the active length of the muscle the exerted force is defined (Relation 6).

$$F_m = f(l_{eff}) \quad (6)$$

The value of the force is depending on the effective length of the muscle and of the pressure of the injected air. The characteristic curves for the exerted forces are represented in Figure 3

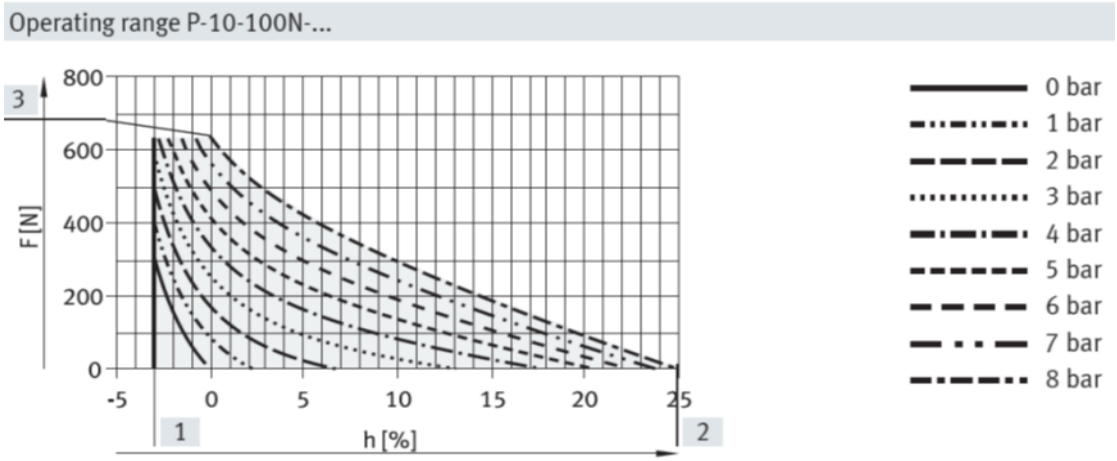

Fig. 3: Force developed by the artificial muscle.

Then, the tangential force F_t is calculated

$$F_t = F_m \cdot \sin\varphi \quad (7)$$

which determines the developed torque

$$M = F_t \cdot r \quad (8)$$

The mechanical power of the engine becomes

$$P_{mech} = M \cdot \omega \quad (9)$$

and its time integral gives the produced mechanical work

$$W_{out} = \int_0^t P_{mech}(t)dt \quad (10)$$

3. Parameters of the engine

A real physical system is considered as well for the simulation given in the next section as for the realized experimental set-up which will be described in section 6. Two artificial muscles of the type DMSP-10-100N are used from which the force-displacement characteristics have already been given through Figure 3. For an operating pressure of 5 bar, the contraction length is equal to 20% of the nominal length of the active part. Then the parameters of the engine are summarized in Table 1.

4. Simulation of the system

The engine described through the kinematic model of the previous section can be simulated in order to evaluate the waveforms and the quantitative values of the different variables. First the effective length of the PAM's is determined in function of the rotational angle φ of the engaged clutch bearings. The engagement occurs when the intake valve of the PAM is opened and the force acts on the lever. The value of the action angle corresponds to the angle j_0. Figure 4 shows the effective lengths of the active part of the PAMs, for the first and the second half-period of the motor cycle, corresponding to the action of the PAM Nr. 1 and 2 respectively.

Table 1: Parameters of the engine.

Muscle type		DMSP-10-100N
Nominal length l_n		0.1m
Diameter of the muscle D_0		0.01m
Mounting end l_2		0.036m
Anchoring rotule l_{rot}		0.036m
Contraction length Dl (5bar)		0.020m
Radius of gyration (lever arms) r		0.018m

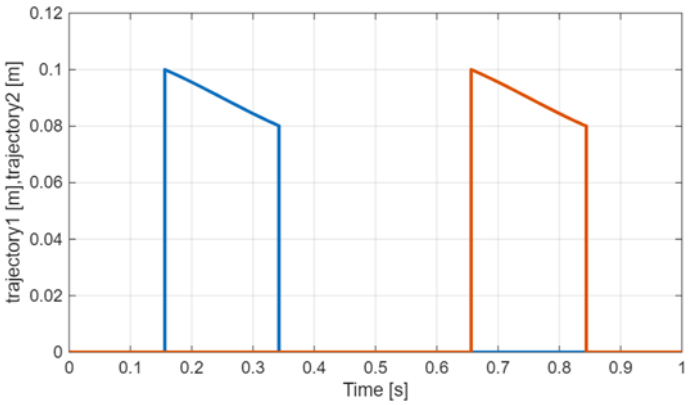

Fig. 4: Effective lengths of the active part of the PAMs Blue: PAM Nr. 1, red: PAM Nr. 2.

From the effective lengths the produced forces of the muscles is calculated. The relation between the effective length and the force corresponds to the curve given in Figure 5. The value of the forces is given as a function of the relative length of the PAM [p.u.]. Figure 6 shows the forces acting in parallel to the PAM's longitudinal axis, F_{m1} and F_{m2}, and also the projection of these forces on a tangential axis to the rotating lever arms, F_{t1} and F_{t2}.

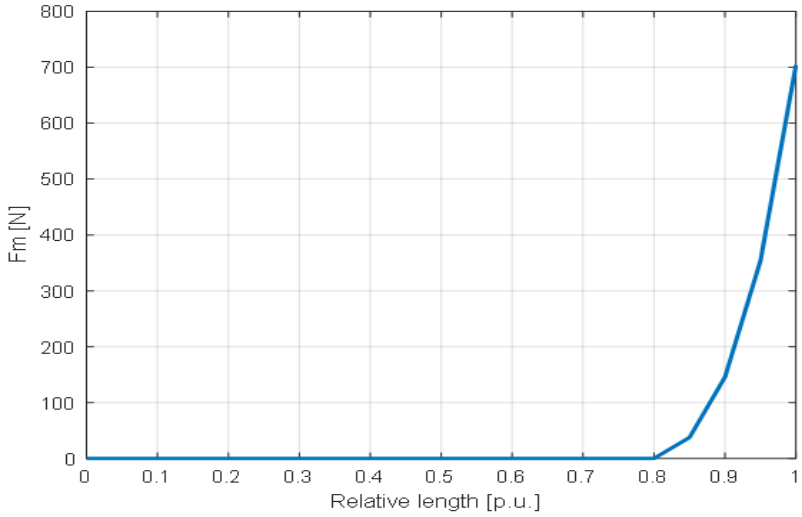

Fig. 5: Approximated form of the function for the force exerted by the muscle.

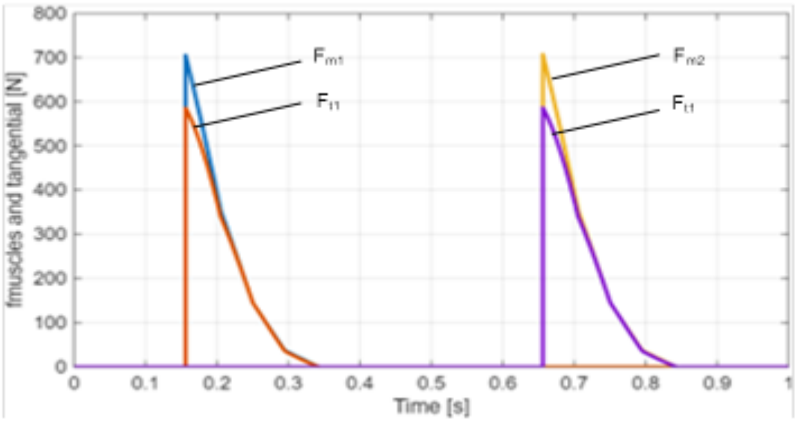

Fig. 6: Longitudinal and tangential forces of the PAM's.

Then the developed torque is calculated (Relation 8). The torque curve is given in Figure 7. From the torque, the

produced power is given through Relation 9. The power curve is given in Figure 8. The strong intermittency of the torque curve already indicates that an inertial element will need to be coupled to the motor shaft to obtain a relatively smooth rotational speed. In the simulation task, a constant rotational speed is considered.

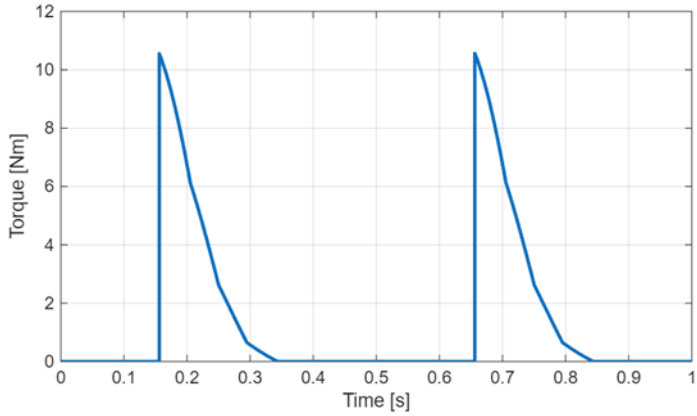

Fig. 7: Torque developed by the engine.

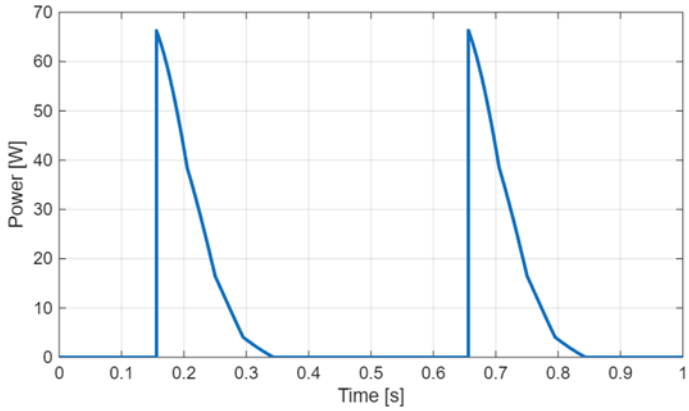

Fig. 8: Mechanical power produced by the motor.

In the next section the energetic efficiency is evaluated. The efficiency must consider the produced mechanical work by the motor. This amount is obtained by a time-integration of the power curve (Relation 10). The corresponding curve is given in Figure 9.

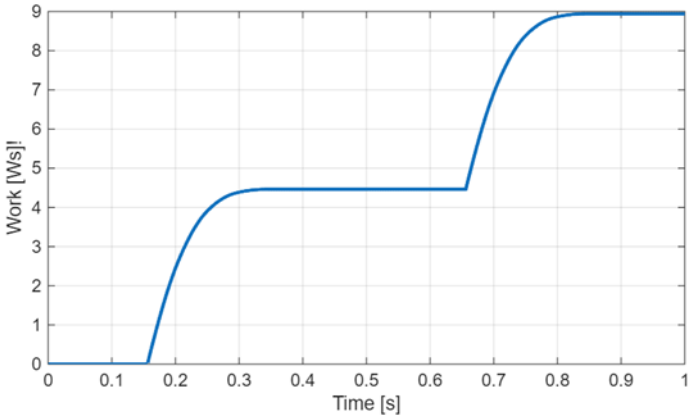

Fig. 9: Produced mechanical work by the motor.

5. Efficiency of the engine

As mentioned in the introduction to this article, manufacturers of pneumatic artificial muscles (PAMs) claim that their devices generate significant tractive forces with minimal compressed air consumption. Therefore, the energy efficiency of PAM based engines is expected to be high. In reality, the actual efficiency is considerably lower, as demonstrated in this section. To evaluate the energy efficiency of an air engine, the ratio of the mechanical work produced, W_{out}, to the enthalpy, H_{in}, of the injected air is calculated (Relation 11).

$$\eta_{conv} = \frac{W_{out}}{H_{in}} = \frac{W_{out}}{U + P_{in} \cdot \Delta V} \tag{11}$$

The value of the produced mechanical work W_{out} is obtained from the integration of the instantaneous power P_{mech} over one period of the motor cycle

$$W_{out} = \int_0^t P_{mech}(t)dt \tag{12}$$

where P_{mech} is the product of the torque multiplied by the angular velocity

$$P_{mech} = M \cdot \omega \tag{13}$$

From the simulation results given in Figures 9 the numerical value of $W_{out} = 8.99J$ is obtained.

For the evaluation of the enthalpy injected into the PAM's, their volume in the pressurized state must be evaluated. Figure 10 gives the dimensions of the PAM under relaxed and contracted conditions.

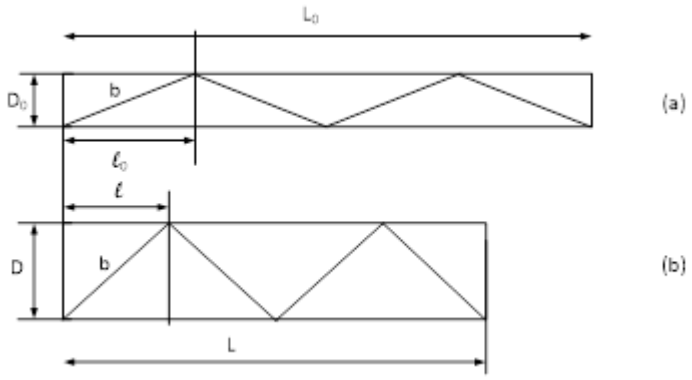

Fig. 10: Dimensions of the PAM.
a) Relaxed state
b) Contracted state

The volume of the pressurized PAM is given by

$$V = \frac{\pi D^2}{4} L \tag{12}$$

where L and D are the length and the diameter of the PAM in its pressurized state

The diameter D is calculated with the assumption that the fiber-length of the mesh are of constant length (parameter b in Figure 10).

From the drawing of the relaxed state (Figure 10a), and if there are 4 "half-turns" of the twine braids over the length of the muscle, b is calculated as

$$b = \sqrt{l_0^2 + D_0^2} = \sqrt{(L_0/4)^2 + D_0^2} \tag{13}$$

and the diameter D of the contracted (pressurized) PAM is

$$D = \sqrt{b^2 - l^2} = \sqrt{b^2 - (L/4)^2} \tag{14}$$

$$U = E_{comp} = P_{in} \cdot V_1 \left(\ln \frac{P_{in}}{P_{atm}} - 1 + \frac{P_{atm}}{P_{in}} \right) \tag{15}$$

Numerically, and considering the complete cycle (j =0…2□) during which two fillings of the PAM's occur with air at 4 bar, U becomes

$$U = E_{comp} = 4 \cdot 10^5 N/m^2 \cdot 40.7 \cdot 10^{-6} m^3 \left(\ln \frac{4bar}{1bar} - 1 + \frac{1bar}{4bar} \right) = 10.36J \tag{16}$$

and

$$P_{in} \cdot \Delta V = 4 \cdot 10^5 N/m^2 \cdot 40.7 \cdot 10^{-6} m^3 = 16.28J \tag{17}$$

Finally, the energetic efficiency becomes

$$\eta_{conv} = \frac{W_{out}}{H_{in}} = \frac{8.99J}{10.36J + 16.28J} = 0.338 \tag{18}$$

6. Experimental set-up

An experimental set-up has been realized on the base of the parameters given in Table 1. The set-up is shown in Figure 11. The two artificial muscles can be seen in the centre of the figure together with the control valves. On the left side the fixed anchors of the muscles and on the right side the connection to the motor shaft through the freewheel lever arms. At the front of the motor shaft the flywheel disk can be seen. A dedicated video shows the real-time operation of the engine [17].

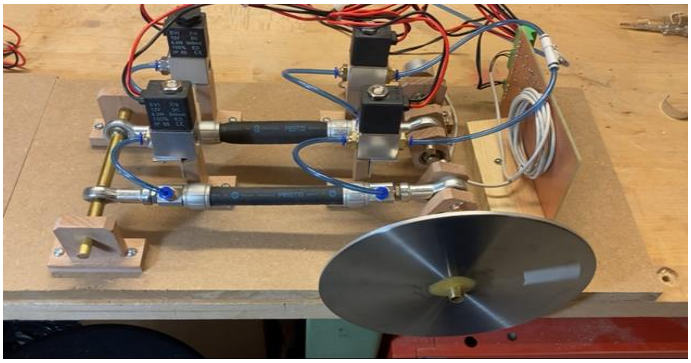

Fig. 11: Experimental set-up.

Conclusion

The concept of a new compressed air engine driven by pneumatic artificial muscles has been verified. The originality of the studied motor is the coupling concept of the PAM's to the motor axle through short lever arms and freewheeling clutch bearings. The coupling concept could be verified, and the energetic efficiency has been evaluated.

References

1. Rufer, A., Energy storage-Systems and components, CRC Press, Taylor & Francis group, Boca Raton FL, November 2017
2. Devang Marvania, Sudhakar Subudhi, A comprehensive review on compressed air powered engine, Renewable and Sustainable Energy Reviews, Volume 70, 2017, Pages 1119-1130, ISSN 1364-0321, https://doi.org/10.1016/j.rser.2016.12.016. (https://www.sciencedirect.com/science/article/pii/S1364032116310681).
3. Atlas Copco, Pocket guide to air motors, 9833 9067 01 2015:1 Jetlag/Boardwalk. Printed in Sweden. © Atlas Copco Industrial Technique AB.
4. Dhumal, A., Ambhore, N., Naik, A. *et al.* Design and Optimization of Air Motor with Gear Rotor System for Enhanced Performance. *J. Inst. Eng. India Ser. C* 106, 367–376 (2025). https://doi.org/10.1007/s40032-024-01157-6.
5. Rufer, A., A High Efficiency Pneumatic Drive System Using Vane-Type Semi-Rotary Actuators, Facta Universitatis, Series: Electronics and Energetics Vol. 34, No 3, September 2021, pp. 415-433, https://doi.org/10.2298/FUEE2103415R.
6. Rufer, A., A High Efficiency Pneumatic Motor Based on Double-Acting Linear Cylinders, World Wide Journal of Multidisciplinary Research and Development, WWJMRD, 2021, 7(1), 25-36.
7. Rufer, A., A four-cylinder pneumatic expansion motor with high efficiency, Academia Green Energy, 2(2), April 2025, DOI: 10.20935/AcadEnergy7625.
8. Rufer, A., Semi-Rotary and Linear Actuators for Compressed Air Energy Storage and Energy Efficient Pneumatic Applications, Bentham Science Publishers Pte, Ltd, Singapore, 2023, ISBN 978-981-5179-11-8.
9. Koruku, S., Samtas, G., Soy, G., Design and Experimental Investigation of Pneumatic Movement Mechanism Supported by Mechanic Cam and Crank Shaft, TEM Journal, Volume 4 / Number 1 / 2015, www.temjournal.com.
10. Kanchana Crishan Wickramatunge, Thananchai Leephakpreeda, Study on mechanical behaviors of pneumatic artificial muscle, International Journal of Engineering Science 48 (2010) 188–198, Elsevier.
11. FESTO, Fluidic muscle, https://ftp.festo.com/Public/PNEUMATIC/SOFTWARE_SERVICE/Documentation/2020/DE/DMSP-MAS_DE.PDF.
12. Chivu, C., Static Model and Simulation of a Pneumatic Artificial Muscle, International conference on Economic Engineering and Manufacturing Systems, Brasov, 25-26 October 2007, https://recentonline.ro/021/Chivu_Catalin_01a-R21.pdf.
13. Wafaa Al-Mayahi, Hassanin Al-Fahaam, A Review of Design and Modeling of Pneumatic Artificial Muscle, Iraqi Journal for Electrical and Electronic Engineering, 2024, https://doi.org/10.37917/ijeee.20.1.13.
14. Hao Zheng, Xiangrong Shen, Double-Acting Sleeve Muscle Actuator for Bio-Robotic Systems, *Actuators* 2013, *2*, 129-144; doi:10.3390/act2040129
15. Rufer, A., Compressed Air Engine based on Pneumatic Artificial Muscles (PAM's)
16. Freewheels - Their Functions and Applications https://hard-met.pl/wp-content/uploads/2019/06/Freewheel-Clutch.pdf
17. https://www.youtube.com/watch?v=qvNCnOenXQo